SCIREA Journal of Physics
ISSN: 2706-8862
http://www.scirea.org/journal/Physics
July 12, 2022
Volume 7, Issue 4, August 2022
https://doi.org/10.54647/physics14469

An expanded Tauc absorption equation and its application to detect all energy gaps and transition types in the band diagram of bulk Silicon.

Emmanuel Saucedo-Flores, Rogelio Guerrero Gonzalez
DIP-CUCEI Universidad de Guadalajara
José Guadalupe Zuno No. 48, Industrial Los Belenes, CP 45101 Zapopan, Jalisco, México
Email: emmauel.saucedo@cucei.udg.mx, rogelio.guerrero4397@alumnos.udg.mx

Abstract

This work presents an expansion of the Tauc absorption model equation by incorporating into it five proportional factors. The new equation is then solved for the original exponent factor, normally having a value chosen among 0.5, 3/2, 2 and 3, which is related to the optical transition type involved in typical photon absorption processes. Plots of the derived expression along a selected photon energy absorbance range allow, by using a properly adjusted set of the four introduced factors, to detect the energy band gap in the local absorbance range and to confirm the guessed optical absorption type of the material under study. The obtained results are validated by comparing the experimental absorbance data trace against the plot of the expanded absorption equation model and against the energy band diagram, if available, of the material under study. Repeating this process for other segments of the absorbance data provides additional band gaps and absorption types whose nature can be correlated with existing models of energy bands diagrams of the investigated material. The proposed method is applied to bulk Silicon.

Keywords: Photon absorption, Tauc equation, electron transition types, energy band diagram, band gap, Urbach absorption tail.

Introduction

The Tauc material optical analysis method [1-7] is based in the expression

$$\alpha = A\frac{(E_{ph}-E_g)^r}{E_{ph}} \text{ (1/cm)} \tag{1}$$

where α (1/cm) is the material absorbance for photons having an E_{ph} (eV) energy supposed to be higher than the material band gap Eg (eV), r is a sort of an absorption activation factor determined by the electron transition type from the valence band to the conduction band and A (eV^{1-r}/cm) is a constant. The two most common r values are 1/2 and 2 which correspond to band to band direct allowed transition, or DAT, which have no phonon involvement and electron keeps its wave vector, and band to band indirect allowed transitions, or IAT, which require a photon/phonon pair to act upon an electron so it undergoes a wave vector change in its transfer process, respectively.

The main use of (1) is actually in the form

$$(\alpha E_{ph})^{1/r} = A^{1/r}(E_{ph}-E_g) \quad (\text{eV/cm})^{1/r} \tag{2}$$

whose left terms plots are used to extract the material band gap by extrapolating the trace into the energy axis which implies an ideal zero absorbance condition.

Expanded Tauc equation and the *r* function

Let's rewrite (1) as follows

$$\alpha = Ae^{BE_{ph}^D}\frac{(CE_{ph}-E_{seed})^r}{E_{ph}^m} \text{ (1/cm)} \tag{3}$$

where A (eV^{m-r}/cm), B (1/eV), C, D, E_{seed} (eV) and m are constants whose intended purpose is to provide a better absorbance model fit; the E_{seed} parameter is not an energy gap, it can even be zero or negative and must comply with $E_{seed} < CE_{ph}$. Observe that (1) is obtained from (3) with the proper choice of the introduced parameters.

Now, rearranging (3) as follows

$$\frac{\alpha E_{ph}^{m}}{Ae^{BE_{ph}^{D}}} = (CE_{ph} - E_{seed})^{r} \ \ (\mathrm{eV})^{r} \tag{4}$$

taking the logarithm on both sides and solving for r gives

$$r(E_{ph}) \equiv abs\left(\frac{\ln(\alpha E_{ph}^{m} / Ae^{BE_{ph}^{D}})}{\ln(CE_{ph} - E_{seed})}\right) \tag{5}$$

where the absolute value was introduced for plotting purposes.

The equivalent expression for (2) in this model is as follows

$$(\alpha E_{ph}^{m})^{1/r} = (Ae^{BE_{ph}^{D}})^{1/r}(CE_{ph} - E_{seed}) \quad (\mathrm{eV}^{m}/\mathrm{cm})^{1/r} \tag{6}$$

Plotting the *r* function for the bulk Si absorbance

Figure 1*a*) shows a plot of the bulk Silicon absorbance raw data obtained from [8] with its smallest energy gap $Eg_{\text{B-Si}}$ = 1.12 eV indicated. Figure 1*b*) depicts the Silicon energy band system, [9], with its band gap demarked by the two horizontal dashed lines, the top one corresponding to the deepest point of the conduction band, E_C, located near the X *k*-vector coordinate while the bottom one is defined by the two valence band, E_V, highest points located at the two Γ *k*-vector coordinates; the gap is identified by the smallest arrow and by the number 1. This and six other wider band gaps arrow-identified in Figure 1*b*) will be studied with (5) including an extra case related to trap assisted electron transitions also known as Urbach tail absorption which is characterized by having r = 1. This electron transition mechanism is not identified in Figure 1.

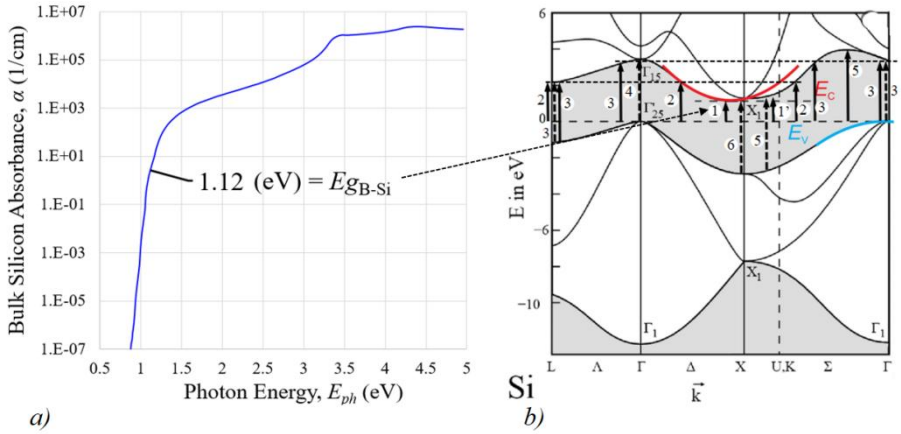

Figure 1. *a*) Photon energy dependence of the absorbance in bulk Si whose main energy gap $Eg_{\text{B-Si}}$ along with six others will be analyzed with the *r* function and will be correlated to the Si energy-wavevector band configuration shown in *b*)[9].

The type of plots that can be produced by the use of expression (5) is exemplified in Figure 2*a*) for the case of detecting the bulk Si smallest band gap $Eg_{\text{B-Si}}$ = 1.119 eV and its associated absorption exponent parameter *r* which happens to be equal to 2 and is well known to be associated to electron band to band indirect allowed transitions (IAT). Note that the obtained band gap energy is referred to (6) and raw data *α* curves.

The $r(E_{ph})$ function plotting process is made along with the absorption model fit (3) trace which is compared to the original absorption curve, see Figure 2*b*); this requires the adjustment of the other six colocation constants to find an $r(E_{ph})$ peak and then one of them - normally A or B - is fine-tuned to increase the peak length while keeping a good model fit for the local absorption data.

Further down, we will address the small peak which appears at the right of Figure 2*a*).

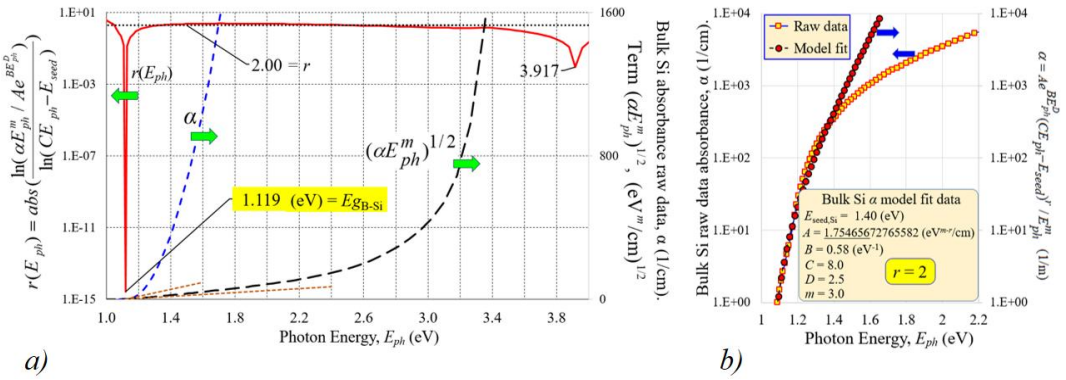

Figure 2. *a*) Use of the $r(E_{ph})$ function (5) to detect the bulk Si main band gap, Eg_{Si}, = 1.119 eV and its absorption exponent parameter value *r* = 2 corresponding to IAT; for the sake of comparison, the obtained peak location is referred to (6) and raw data *α* curves. *b*) Absorbance raw data and its model fit with used parameters in the $r(E_{ph})$ plot. If parameter A non-underlined digits are dropped, the trace peak is reduced to about half in length.

Figure 3*a*) gives the $r(E_{ph})$ plot corresponding to the detection of the next band gap indicated in Figure 1*b*) as 1' and with the arrow located near of the U, K *k*-vector coordinate. It's identified as $Eg'_{\text{B-Si}}$, is equal to 1.172 (eV) and has an *r* = 2 with IAT nature also. Figure 3*b*) compares the obtained absorption model fit to the local raw data.

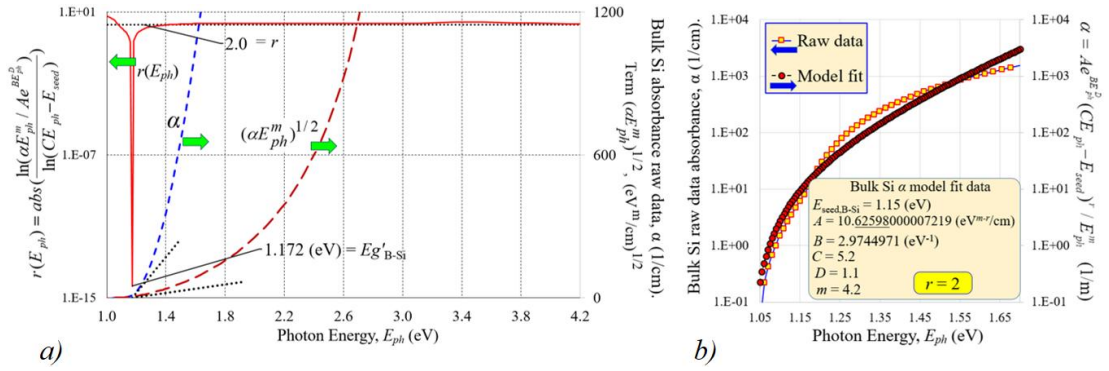

Figure 3. *a*) $r(E_{ph})$ function used to detect a Si band gap of Eg'_{Si} = 1.172 eV with absorption exponent parameter value also of r = 2 corresponding to IAT. *b*) Absorbance raw data and its model fit with used parameters in the $r(E_{ph})$ plot.

At the L k-vector coordinate of Figure 1*b*) there is a band gap identified as 2 and the leftmost solid arrow whose detecting $r(E_{ph})$ plot is presented in Figure 4*a*). It's named as $Eg_{2B\text{-}Si}$, is equal to 2.103 (eV) and has an r = 2 with IAT nature also; note that in Figure 1*b*) there are two other solid arrows also identified as 2 and corresponding also to IAT. Again, the obtained band gap energy is referred to slops along (6) and raw data α curves. The obtained absorption model fit to the local raw data is shown in Figure 4*b*). Note that, for this case, to the left of the $r(E_{ph})$ peak in Figure 4*a*), r = 2 as detected in Figure 3*a*) for the same photon energy range.

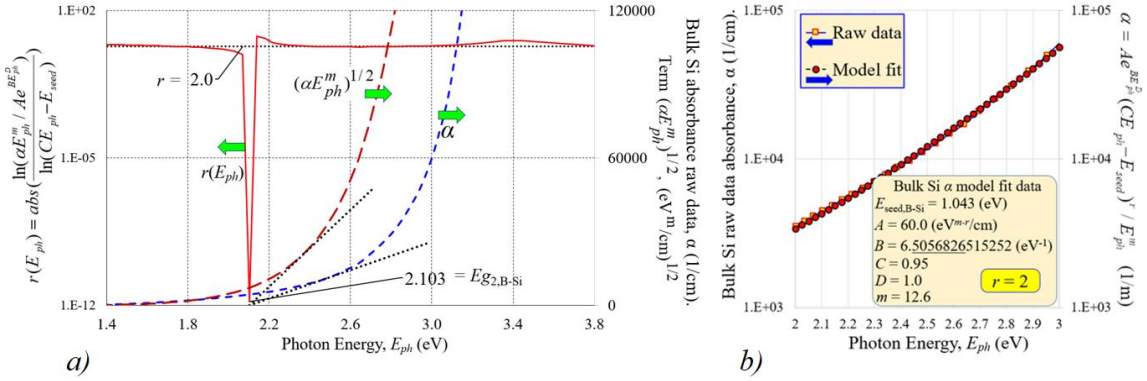

Figure 4. *a*) Detection of the bulk Si band gap, $Eg_{2,Si}$ = 2.103 eV and its absorption exponent parameter value r = 2 corresponding to IAT. *b*) Involved local absorbance raw data and its obtained model fit comparison.

The two dashed arrows identified with a 3 and shown at the right and at the left edges of Figure 1*b*) are of the same length and are expected to correspond to an r = 0.5 with DAT. There are other four solid arrows also identified as 3 and have the same gap width but correspond to an r = 2 with IAT. In Figure 5*a*), the $r(E_{ph})$ function detects this gap. It's identified as $Eg_{3B\text{-}Si}$ and is equal to 3.208 (eV). This time, the involved absorption process shows a dual nature; it starts having an r = 2 with an IAT behavior and then changes into r =

0.5 for a DAT nature. As above, at the left of the $r(E_{ph})$ peak in Figure 5*a*), $r = 2$ as observed in Figure 4*a*) for the same photon energy range.

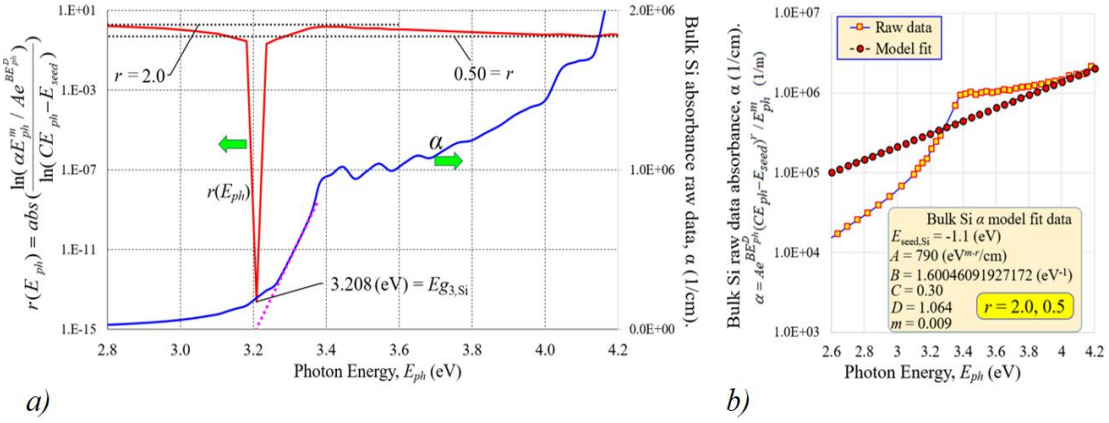

Figure 5. *a*) The bulk Si third band gap, $Eg_{3,Si}$, = 3.208 eV detection showing that its absorption exponent parameter has a dual nature with an $r = 2$ corresponding to IAT and also an $r = 0.5$ for DAT. *b*) Involved local absorbance raw data and its obtained model fit comparison.

The band gap identified as 4 and has a dashed arrow, see the left Γ *k*-vector coordinate of Figure 1*b*), is determined in Figure 6*a*), named as $Eg_{4B\text{-}Si}$ and is of 3.265 (eV) wide. The local valence and conduction bands configuration establishes clear conditions for direct allowed transitions with $r = 0.5$ which is the case shown in Figure 6 *a*). Figure 6*b*) plots the obtained absorbance model fit and gives all the introduced parameters. Despite that the band gap $Eg_{3B\text{-}Si}$ is too close to $Eg_{4B\text{-}Si}$ peak in Figure 6*a*), $r = 0.5$ and $r = 2$ regions are detected at the left side of Figure 6*a*) as for the same photon energy range in Figure 5*a*) and Figure 4*a*).

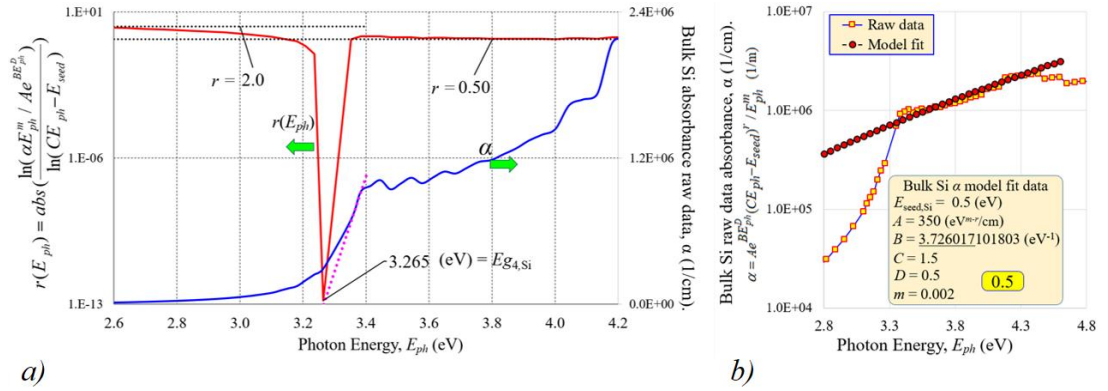

Figure 6. *a*) Use of the $r(E_{ph})$ function to detect the bulk Si third band gap, $Eg_{4,Si}$, = 3.265 eV and its absorption exponent parameter value $r = 0.5$ corresponding to DAT: observe the small absorption segment associated to the detected threshold photon energy . *b*) Involved local absorbance raw data and its obtained model fit comparison.

The band gap number 5 in Figure 1*b*) has two arrows, one is solid, related to indirect allowed transitions, and the other is dashed, corresponding to direct allowed transitions. The $r(E_{ph})$

function analysis in Figure 7*a*) provides $Eg_{5B\text{-}Si}$ = 3.837 (eV) and detects a dual nature absorption mechanism with r = 0.5 corresponding to DAT and r = 2.0 for IAT. Again note that, at the left side of Figure 7*a*), r = 0.5 as obtained in Figure 6*a*) for the same photon energy range.

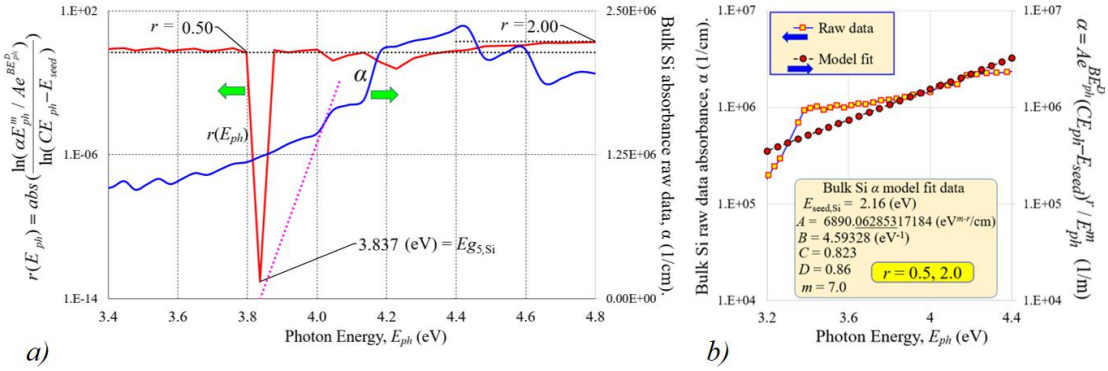

Figure 7. *a*) Use of the $r(E_{ph})$ function to detect the bulk Si fifth band gap, $Eg_{5,Si}$, = 3.837 eV and its absorption exponent parameter dual value r = 0.5 corresponding to DAT and r = 2.0 for IAT; again, a tiny absorption segment is used to refer this threshold photon energy. *b*) Involved local absorbance raw data and its obtained model fit comparison.

Number 6 band gap is the wider one in Figure 1*b*); its local $r(E_{ph})$ function in Figure 8*a*) detects a gap width of $Eg_{6B\text{-}Si}$ = 3.959 (eV) and, as expected from the site configuration of the valence and conduction bands, it calls for energy wise early photons to produce only direct allowed transitions with r = 0.5 while indirect allowed transitions with r = 2 become also present for higher energy photons. The used parameters for the absorbance model fit are shown in Figure 8*b*). A curious note here is that the energy value 3.917 at the edge of peak detection was also present in Figure 2*a*).

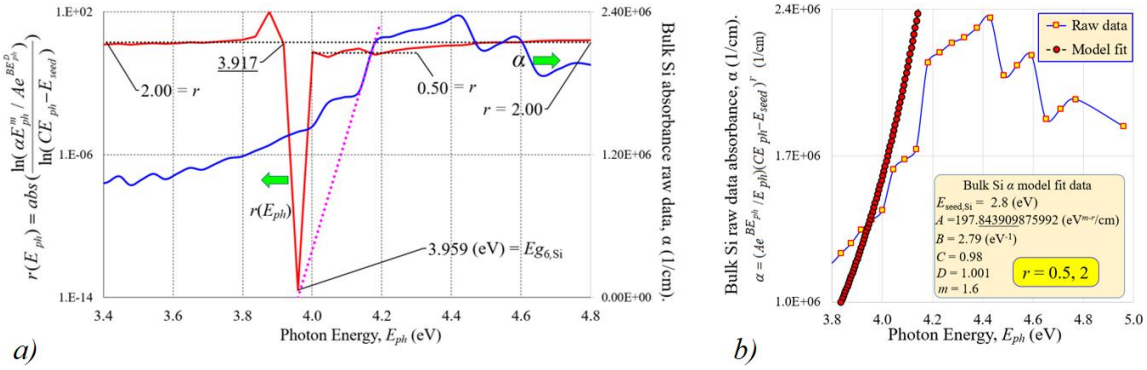

Figure 8. *a*) Use of the $r(E_{ph})$ function to detect the bulk Si fifth band gap, $Eg_{6,Si}$ = 3.959 eV; its absorption exponent parameter shows a dual value behavior, namely r = 1/2 and r = 2 corresponding to DAT and IAT, respectively; note the absorption segment associated to the detected threshold photon energy. *b*) Involved local absorbance raw data and its obtained model fit comparison.

The trap assisted Urbach absorption energy peak for bulk Si

The bulk Silicon absorbance plot in Figure 1*a*) shows a segment of absorption for photon energies under the main $Eg_{B\text{-}Si}$ gap which is associated to impurities and lattice defects assisted electron transitions. Impurities and defects create energy levels referred to as traps which give rise to what is called Urbach tail absorption; these electron transitions can occur in three different ways: 1) from the valence band to an empty trap, 2) from a filled trap to the conduction band and 3) from a filled trap to an empty trap. These optical processes are associated to an r value of 1.

The $r(E_{ph})$ function to detect the Urbach tail energy peak is plotted in Figure 9*a*). It has a value of $Eg_{B\text{-}Si}$ = 0.986 eV and presents an r = 1. Figure 9*b*) depicts the model fit for the local absorbance raw data.

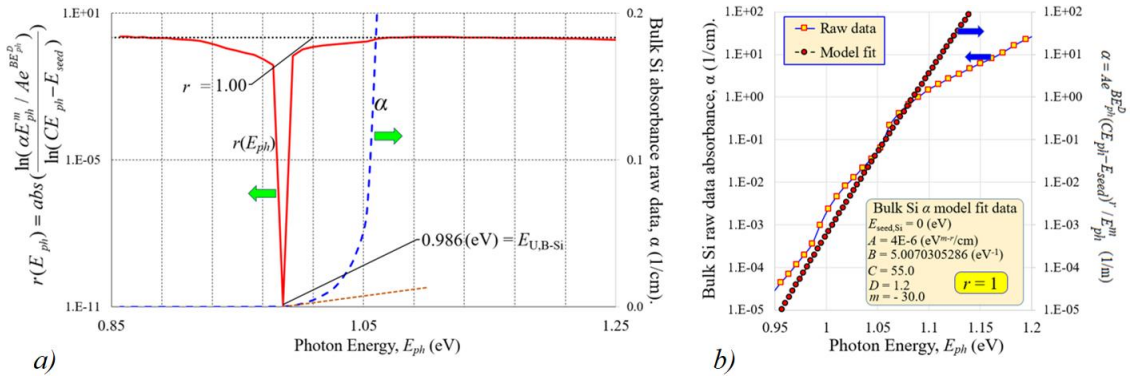

Figure 9. *a*) Detection of bulk Si trap assisted Urbach tail optical transitions energy peak, $E_{U,B\text{-}Si}$, and optical transition type r = 1. *b*) Local absorbance raw data and model fit for involved parameters.

Summary and conclusion

The energy gap values obtained using the proposed $r(E_{ph})$ function are summarized in Figure 10*a*) along with their respective electron transition r value or values in some cases. Figure 10*b*) is a simplified band diagram of Si with a couple of yellow rectangles to represent the non-continuous trap levels involved in the Urbach tail absorption case; all gaps discussed above are represented at all sites where their corresponding energy threshold might provide local absorption activity. Both bands are segmented in regions to help understand the electron transitions among them. For example, if a photon with energy E_{ph} such that $1.12 = Eg \leq E_{ph} \leq Eg_2 = 2.1$ (eV) is absorbed along with a phonon of the proper wavevector by an electron in regions identified as I in the valence band, the only possible electron destiny is to land in region A of the conduction band.

This will be also the case for a photon with energy E_{ph} such that $Eg_6 \leq E_{ph} \leq Eg_6 + Eg_2 - Eg$ (eV) absorbed along the whole region V of the valence band, the excited electron can transit only into the region A of the conduction band; however, this time the particle transition can either be direct or indirect as detected in the $r(E_{ph})$ function in Figure 8*a*).

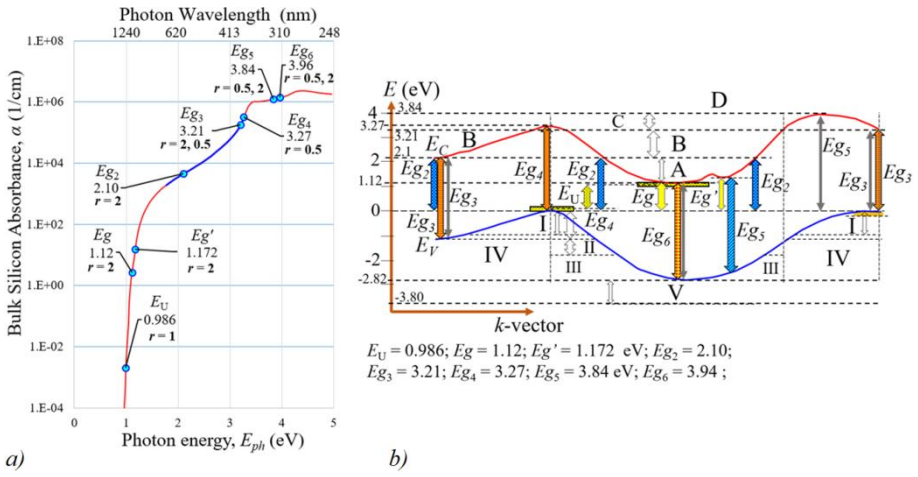

Figure 10. *a*) Summary of the detected optical transition photon energy thresholds for the Bulk-Si absorbance. *b*) Schematics of the Si energy band system showing possible energy-wise early top localization in the valence band of the values shown in *a*).

The bottom of the two B regions in the conduction band have three photon energy thresholds related to energy gap Eg_2 = 2.1 eV while its top line is established by the energy gap Eg_3 = 3.21 eV. Photons within these two energy values which are absorbed along the slightly extended regions I in the valence band will produce exclusively electron indirect transitions into B regions; this is confirmed by the $r(E_{ph})$ trace in Figure 4*a*). $r(E_{ph})$ plots in Figures 3*a*), 5*a*), 6*a*), 7*a*) and 8*a*) can be similarly associated to the involvement of regions identified in Figure 10*b*) for corresponding energy gap *Eg*', Eg_3, Eg_4, Eg_5 and Eg_6, respectively, while the energy peak in E_U case in Figure 9*a*) is associated to the trap levels present in the yellow colored rectangles just outside the two bands; the dimensions of these rectangles are arbitrary.

In summary, it has been shown that the proposed expanded $r(E_{ph})$ expression provides a good alternative to Tauc's equation for the sake of extracting useful properties of materials out of their optical absorption data. The authors have already successfully tested the method in acrylic sheets and in dissolved nanoparticles.

Acknowledgments

The authors express their appreciation for the financial support received from the Universidad de Guadalajara (ESF) and from the Mexican Consejo Nacional de Ciencia y Tecnología (RGG).

References

[1] J. Tauc, R. Grigorovici, A. Vancu,Optical Properties and Electronic Structure of Amorphous Germanium, Phys. Status Solidi Basic Res. 15 (1966) 627–637. TaucRef1

[2] J. Tauc, Optical properties and electronic structure of amorphous Ge and Si, Mat. Res. Bull. 3 (1968) 37–46. TaucRef2

[3] J.H. Chu, Z.Y. Mi, D.Y. Tang, Band-to-band optical absorption in narrow-gap Hg1-xCd xTe semiconductors, J. Appl. Phys. 71 (1992) 3955–3961. https://doi.org/10.1063/1.350867.

[4] B.D. Viezbicke, S. Patel, B.E. Davis, D.P. Birnie, Evaluation of the Tauc method for optical absorption edge determination: ZnO thin films as a model system, Phys. Status Solidi Basic Res. 252 (2015) 1700–1710. https://doi.org/10.1002/pssb.201552007.

[5] N. Sangiorgi, L. Aversa, R. Tatti, R. Verucchi, A. Sanson, Spectrophotometric method for optical band gap and electronic transitions determination of semiconductor materials, Opt. Mater. (Amst). 64 (2017) 18–25. DOI#5 .

[6] R. Guerrero-Gonzalez, F.A. Orona, E. Saucedo-Flores, R. Ruelas, J.E. Pelayo-Ceja, R. Lopez-Delgado, A. Cordova-Rubio, M.E. Álvarez-Ramos, A. Ayon, Synthesis of Si and CdTe quantum dots and their combined use as down-shifting photoluminescent centers in Si solar cells, Mater. Renew. Sustain. Energy. 8 (2019) 1–8. https://doi.org/10.1007/s40243-019-0153-0

[7] J.C. Melendres-Sánchez, R. López-Delgado, G. Saavedra-Rodríguez, R.C. Carrillo-Torres, R. Sánchez-Zeferino, A. Ayón, M.E. Álvarez-Ramos, Zinc sulfide quantum dots coated with PVP: applications on commercial solar cells, J. Mater. Sci. Mater. Electron. 32 (2021) 1457–1465. https://doi.org/10.1007/s10854-020-04916-0 .

[8] Optical Properties of Silicon | PVEducation, (n.d.). SiliconAbsorbance (last accessed April 7, 2022).

[9] Figure used by Helmut Föll and Jürgen Carstensen gentility, "Free quantum mechanical particles and band structure". BandDiagram (last accessed April 7, 2022).